2015

Application and Histology-Driven Refinement of Active Contour Models to Functional Region and Nerve Delineation: Towards a Digital Brainstem Atlas

Nimal Patel
Old Dominion University

Sharmin Sultana
Old Dominion University

Tanweer Rashid
Old Dominion University, trashid@odu.edu

Dean Krusienski
Old Dominion University, djkrusienski@vcu.edu

Michel A. Audette
Old Dominion University, maudette@odu.edu

Original Publication Citation

Patel, N., Sultana, S., Rashid, T., Krusienski, D., & Audette, M. A. (2015). Application and histology-driven refinement of active contour models to functional region and nerve delineation: Towards a digital brainstem atlas. In Z. R. Yaniv & R. J. Webster, III (Eds.), *Medical Imaging 2015: Image Guided Procedures, Robotic Interventions, and Modeling, Proceedings of SPIE Vol. 9415* (94150I). SPIE, Bellingham, WA. https://doi.org/10.1117/12.2082400

Application and histology-driven refinement of active contour models to functional region and nerve delineation: towards digital brainstem atlas

Nirmal Patel[b], Sharmin Sultana[a], Tanweer Rashid[a], Dean Krusienski[b], Michel A. Audette[a]
[1:] Department of Modeling, Simulation and Visualization Engineering, Old Dominion University
[2:] Department of Electrical and Computer Engineering, Old Dominion University

ABSTRACT

This paper presents a methodology for the digital formatting of a printed atlas of the brainstem and the delineation of cranial nerves from this digital atlas. It also describes on-going work on the 3D resampling and refinement of the 2D functional regions and nerve contours. In MRI-based anatomical modeling for neurosurgery planning and simulation, the complexity of the functional anatomy entails a digital atlas approach, rather than less descriptive voxel or surface-based approaches. However, there is an insufficiency of descriptive digital atlases, in particular of the brainstem. Our approach proceeds from a series of numbered, contour-based sketches coinciding with slices of the brainstem featuring both closed and open contours. The closed contours coincide with functionally relevant regions, whereby our objective is to fill in each corresponding label, which is analogous to painting numbered regions in a paint-by-numbers kit. Any open contour typically coincides with a cranial nerve. This 2D phase is needed in order to produce densely labeled regions that can be stacked to produce 3D regions, as well as identifying the embedded paths and outer attachment points of cranial nerves. Cranial nerves are modeled using an explicit contour based technique called 1-Simplex. The relevance of cranial nerves modeling of this project is two-fold: i) this atlas will fill a void left by the brain segmentation communities, as no suitable digital atlas of the brainstem exists, and ii) this atlas is necessary to make explicit the attachment points of major nerves (except I and II) having a cranial origin.

Keywords: digital atlas, contour models, surface models, brainstem, cranial nerves.

1. INTRODUCTION

There are a number of digital atlases of the brain in open source, but these atlases neglect the brainstem: they typically represent the whole brain, with little detail provided to the brainstem. The full-brain atlases include Harvard's Surgical Planning Laboratory (SPL) Atlas, atlases available with Oxford's FMRIB Software Library (FSL), which are listed on FSL's wiki [1] and the Freesurfer software package [2, 3]. To our knowledge, none of the digital brain atlases adequately describes the brainstem. The only competing option is the Mai online atlas [4], however its brainstem model is low-resolution and not descriptive enough for our needs, especially in comparison to printed atlases such as the Duvernoy [5] and the Paxinos [6] atlases.

The proximal clinical objective of this project is to provide a minimally supervised segmentation tool for patient-specific modeling of the brainstem. A more long-term objective is to develop a general methodology for transposing any printed atlas, typically derived from expert-labeled histological data, to a dense 3D digital label format. The clinical importance of detailed brainstem model, which can be warped to patient image data, and by extension the patient-specific modeling of cranial and cervical spinal nerves, is multi-faceted. First, several complications have arisen in the past due to iatrogenic damage in the skull base and spine by surgery and radiotherapy, which could have been prevented by more descriptive surgery planning as well as surgery simulation that would have penalized gestures deleterious to these structures. Second, topological variability in the form of anastomoses, or unusual connections, can occur between cervical spinal nerves and cranial nerves, and patient-specific descriptive modeling of the anatomy for planning and simulation must cope with this variability [7].

The brainstem encloses the points of attachment of ten of the twelve pairs of cranial nerves, as depicted in figure 1. It is also the pathway for all fiber tracts passing up and down from peripheral nerves and spinal cord to the upper areas of the brain. It consists of three components: the medulla oblongata, the midbrain and the pons. The medulla oblongata acts as a relay station for motor tracts crossing between the spinal cord and the brain. It exerts control on the respiratory, motor

Medical Imaging 2015: Image-Guided Procedures, Robotic Interventions, and Modeling,
edited by Ziv R. Yaniv, Robert J. Webster III, Proc. of SPIE Vol. 9415, 94150I
 · doi: 10.1117/12.2082400

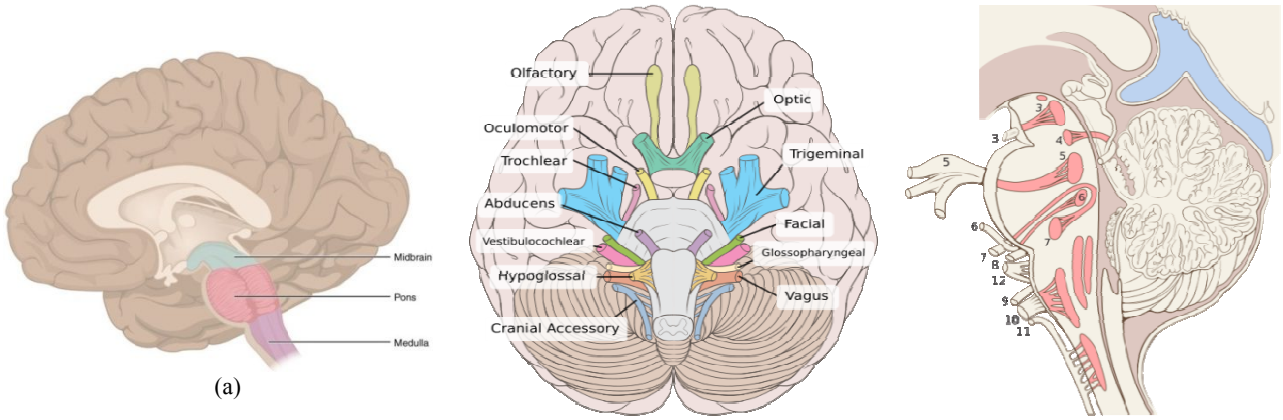

(a) (b) (c)

Figure 1. Anatomy of the brainstem. (a) structure of brainstem, with medulla oblongata adjacent and structurally similar to spinal cord; (b)-(c) cranial nerves, with nerves III (oculomotor) to XII (hypoglossal) having nuclei within, and attachment points on, the brainstem; (b) inferior view; (c) sagittal view with cranial nerve nuclei and tracts inside the brainstem shaded red (reproduced from Wiki of the brainstem and cranial nerves).

and cardiac functions, as well as on several mechanisms of reflex activities such as swallowing and vomiting. The midbrain is the neural pathway of the cerebral hemispheres and contains auditory and visual reflex centers. The pons links different parts of the brain and is the relay station from the medulla to the higher cortical structures of the brain; it also contains the respiratory control center. While it lies in the inferior part of the brain, the brainstem is structurally continuous with the spinal cord. Also, surgery planning and simulation of the spine requires adequate modeling of critical tissues, the most important of which are spinal nerves, and in the cervical portion of the spine, three of these major nerves, the glossopharyngeal (IX), vagus (X) and accessory nerves (XI) run near spinal nerves, while nerve XI has both a cranial and a spinal portion with roots in the brainstem and spine.

Just as importantly, the brainstem is extremely relevant to modeling the neuroanatomy of the skull base. In particular, the brainstem imbeds the nuclei and tracts of ten pairs of cranial nerves, nerves III to XII, and can be thought of as a twenty-legged spider. The olfactory (I) and ocular (II) nerves, emerge from the forebrain anteriorly and superiorly to the brainstem. So far, modeling that is conducive to the minimally supervised segmentation of cranial nerves has been neglected by the computer assisted surgery community.

To enable minimally supervised, highly descriptive, patient-specific identification of cranial and cervical nerves, we argue that a digital atlas for their most prevalent topology must first be developed, as a foundation for modeling variations such as those due to anastemoses. One of the objectives of this brainstem atlas is to serve as cornerstone for the development of a cranial and cervical nerve atlas, which in turn will be used to stabilize the tractographic reconstruction of these nerves from diffusion imaging data, irrespective of their patient-specific topology.

This paper presents a methodology, emphasizing a 2D processing stage while also providing preliminary results in 3D, for the development of a digital atlas of the brainstem including a model of embedded cranial nerves. Our on-going 3D descriptive atlas development will lead to significant improvements, including a representation based on active multi-surface models [8] and 3D active contour models.

2. METHODS

2D Methodology

Our proximal objective is to semi-automatically process a series of input scanned images from a textbook, in order to generate continuously labeled digital images that are suitable for stacking and resampling, to ultimately produce a digital volumetric atlas, featuring functional regions and embedded nerve tracts, suitable for 3D registration with a given patient's brainstem appearing in MRI data. The printed atlas images typically have labeled regions where the labels are numbers centered within them. In order to reduce irregularities within regions, an anisotropic diffusion method was utilized. Our first attempts were centered on the Duvernoy atlas [5], however we determined that its resolution along the

longitudinal (or proximal-distal, or Z) axis was insufficient for our requirements; as a result, we have also begun applying our methods to digitizing the Paxinos atlas, which in turn presented a number of slightly different challenges.

The following methodology is usable when dealing with solid-line contours with numbers within them, but generally not with contours consisting of broken lines. The Duvernoy atlas [5] consists of solid-line contours; the pdf version of the Paxinos atlas available online from its second author [6] and consists of both solid-line and broken-line contours, which motivates the development of a more robust method. Recently, we have found a way to exploit a conversion from pdf to svg. The pdf file of the Paxinos atlas stores contours in a vector format; by replacing all occurrences of "stroke-dasharray" with "stroke-linecap" within the svg file, we found that we could produce solid lines and revert to the basic algorithm. Nonetheless, we are still pursuing a robust methodology that can cope with broken lines as described in the Results and Discussion section.

Basic Algorithm - Paint-by-number Contours

The basic 2D algorithm for full-line contours is follows. Both region-based and gradient-based level set methods were tested. The Chan-Vese region-based model [9] would typically bleed across the boundary of the region, which prompted us to adopt a gradient-based method proposed by Caselles [10], was found to be more reliable for most regions.

The printed atlas images typically have labeled regions where the labels are numbers centered within them. A rectangle that covers an entire label while being inside the boundaries of the corresponding region initializes the contour of the region. This rectangular contour is used to initialize an outwardly moving level sets contour model, whose objective is to propagate a user-supplied label, ostensibly the same number, to boundaries of that region.

In order to reduce irregularities within regions, an anisotropic diffusion method was utilized. Anisotropic diffusion tries to preserve the edges as opposed to isotropic diffusion methods which blurs entire image indiscriminately. The anisotropic function used was modified curvature diffusion equation which is:

$$f_t = |\nabla f| \nabla \cdot c(|\nabla f|) \frac{\nabla f}{|\nabla f|} \tag{1}$$

where f is the image and c is the conductance function .

The level set using Geodesic Active Contours evolves according to the following equation:

$$C_t = g(I)\,(c + k)\,\vec{\mathcal{N}} + \left(\nabla g \cdot \vec{\mathcal{N}}\right)\vec{\mathcal{N}} \tag{2}$$

where $g(I)$ is the stopping function, k is the curvature, and $\vec{\mathcal{N}}$ is curve normal.

The initial level set function was generated using the Fast Marching method [11], in order to produce a computationally efficient label propagation process. The Fast Marching method also requires an initialization, coinciding with the rectangular initialization contour at time t=0 from which the level set model evolves. Our labeling program sets the user-provided rectangular contour as a seed. After the zero level set stabilizes at the region boundary, its propagation domain is colored according to the user-supplied label. As a result, the pixels outside the level set are white whereas the pixels inside the final level set result have the user-supplied value.

Finally, the atlases make the assumption of a vertical axis of symmetry. In our labeling interface, the user supplies a few points that determine this axis. These points determine a segment by regression, and in the event of a small difference rotation with respected to the vertical axis, this rotation is corrected to ensure that the axis of symmetry coincides with the y-axis. A mirror image is then generated by flipping the rotated image about the y-axis. To generate the final image, the mirrored and rotated images are arranged side-by-side such that the mirror image is on the negative side of the x-axis and the rotated image is on the positive side of the x-axis.

Modeling cranial nerves and robust contours with 1-Simplex models

The Duvernoy atlas also features open contours coinciding with cranial nerve paths. To extracts nerves from the labeled regions, it requires user-supplied start and end points and optional mid-points. A shortest path is then calculated from the start point to the end point while crossing the mid points [12]. This shortest path extraction involves the Fast Marching Minimal Path algorithm [13].

For modeling the nerves explicitly, which is needed for 3D segmentation, we have implemented a 1-Simplex model, which is depicted in figure 2 and is the contour version of Delingette's 2-Simplex surface model [14]. An N-Simplex is defined as having (N+1)-connectivity. The 2-Simplex active surface model is well documented as a quasi-Newtonian discrete model for vertex motion, which exhibits 3-connectivity, and has been extensively applied to anatomical boundary segmentation. We have begun using the implementation of the 1-Simplex, characterized by 2-connectivity, for applications in both 2D and 3D. Its advantage over level set contour models is precisely that it retains its topology no matter what, and moreover one can impose greater stiffness on the contour model than with the level-set model approach, which can make it appropriate for preventing bleed-through in broken-line contours.

Our objective for this 1-Simplex model is to produce an explicit contour in 2D, to which we will assign Z-coordinates according to image slices, and refine these 1-Simplex imbedded nerve models with high-resolution histological data. We are using 1-Simplex model as the rough estimation of the nerve centerline. An image- based external energy is then used to deform this model towards the true centerline of the nerves. This image based energy attracts the 1-simplex model towards the points which have high centeredness within the high-vesselness structures. High-vesselness points coincide with points where the eigen-analysis of the local 2D Hessian produces one eigenvalue close to zero and a second much (absolutely) larger eigenvalue [15]. The Minimal Path (MP) can be defined to be weighted such that the lowest-energy path is near points of high-vesselness value. This MP can in turn serve as initialization to a discretized 2-connected contour model that is attracted to the centerline of tubular zones of high-vesselness points, as shown in figure 2(b).

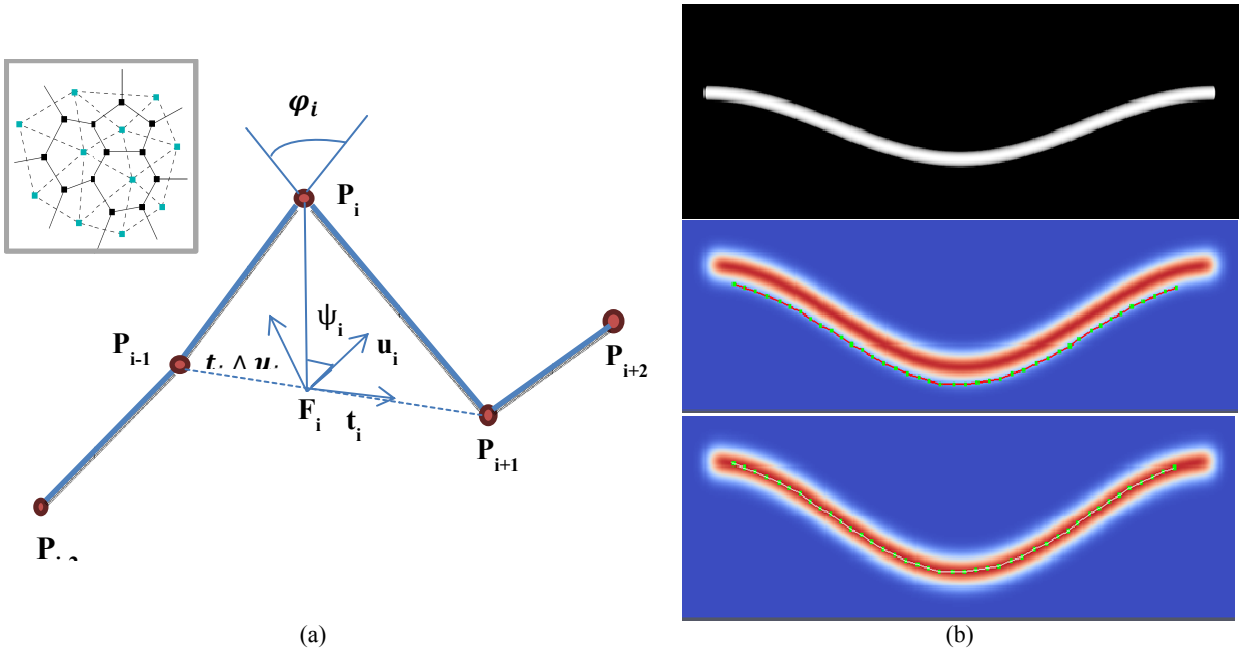

Figure 2. 1-Simplex contour model. (a) Basic topology of 1-Simplex contour model shown for 3D geometry – inset: 2-Simplex topology for surface modeling as pioneered by Delingette (depicted in black, with dual triangulated mesh depicted in blue); (b) basic 2D 1-Simplex applied to tubular synthetic structures – top: tubular image; middle: initialization from nearby vesselness-weighted Minimal Path; final 1-Simplex coinciding with tube centerline.

3D Processing

3D processing is currently underway, and exploits the following methods. First, a preliminary estimate of the Z-coordinate is obtained from a coronal view of the printed atlas, as depicted in figure 3. These Z-coordinates provide cues as to how to stack the 2D label maps, to produce a first version of the 3D label map, as well as what Z-value to assign to putative 2D contours of imbedded cranial nerves. What will follow is an isotropic resampling of the 3D label map, as well as a refinement of 3D open contours of embedded cranial nerves based on intensity values of the high-resolution MNI-space fitted histological data [16], after a global warping of the atlas to the same MNI space.

The dense 3D label map is intended to serve as a first estimate towards a multi-surface model that will be registered with the image of a patient. The basic boils down to the following approach. We will use the stacked images of dense labels to produce a volumetric dense label map, which can be warped to a MRI patient dataset using a suitable registration metric (e.g. mutual information maximization), and then exploit this label map with a multi-material contouring algorithm, currently underway, to produce a multi-surface triangulated boundary of the brainstem atlas.

Briefly, our multi-material dual contouring method, which is still unpublished, is based on the work by Zhang and Qian [17][18], the volume is first subdivided into a uniform grid of an appropriate size. An octree (whose leaves represent the grid cubes) is then used for fast parsing of the grid cubes and polygon generation. Each corner of the grid cube including the center is assigned a material index based on their location in the implicit volume. The dual vertices (also called minimizers) are computed using Quadratic Error Functions (QEFs). In our implementation, we only compute one minimizer for each grid cube. The classical dual contouring method may encounter problems in producing 2-manifold surfaces due to the presence of ambiguous grid cubes. The method of Zhang and Qian [17][18] attempts to resolve the topological inconsistencies inherent in classical dual contouring (DC) by further decomposing the ambiguous grid cubes into 12 tetrahedra. During the polygon generation phase, we follow the classical DC approach by analyzing minimal edges. Each minimal edge is a sign change edge that is shared between four grid cubes.

It should be noted that only the Duvernoy atlas features open contours coinciding with nerves, while the Paxinos atlas does not. Our plan is to co-register the two, so that we obtain the dense voxel labels of the Paxinos atlas in the same space as the explicit representation of the nerves from the Duvernoy. In both cases, 1-Simplex contours and 2-Simplex surfaces, we believe that the high-resolution data of the MNI high-resolution histology data [16] of the brainstem will allow us to capture subtle differences in shape between the printed atlas (and somewhat limited in longitudinal resolution) and a typical human brainstem anatomy. Probabilistic modeling is feasible with the Simplex, as demonstrated by Tejos [19], and we plan to apply this formalism to both the 1-Simplex and 2-Simplex.

3. RESULTS AND DISCUSSION

Currently, we can demonstrate encouraging 2D contour results for both the Duvernoy and Paxinos atlases, as shown in figure 3. By and large, from a subjective level, there is good consistency in the labeling from slice to slice, as can be seen in figure 3(b). There are nonetheless a few inconsistencies, a red region in the third slice coinciding with the position of a yellow region in the fourth slice; we are beginning a collaboration with a neuroanatomy expert who will disambiguate these inconsistencies, as well as orient our adaptations of the atlas to conform from the high-resolution data available in the Big Brain dataset [16]. We believe nonetheless that this exercise with the Paxinos atlas will prove to be tractable, given the exquisite detail of this printed atlas.

Figure 4 features some model-based contouring of a nerve path found in an image of the Duvernoy atlas, which eventually will be co-registered with the Big Brain data and complement the functional information extracted from Paxinos. Our processing of this information begins with the 2D 1-Simplex modeling shown in figure 4(b), on the basis of an initialization in the form of a vesselness-weighted Minimal Path depicted in figure 4(a). This 2D model will be transposed to 3D based on the Z-coordinate obtained from the legend in figure 4(c), which will initialize a fully 3D 1-Simplex as depicted in figure 2(a). We believe that subtle information available in the Big Brain data will allow us to refine the 3D tortuosity that is not apparent given the longitudinally sparse information of the Duvernoy. This implementation is underway.

Figure 5(a) illustrates preliminary results for 3D stacking of 2D Paxinos slices. Figure 5(b) also provides insight on the future work, which will leverage our on-going research on multi-material contouring and multi-surface 2-Simplex modeling. The multi-material contouring, development of which is in the final stages, will produce a collection of triangulated boundaries for the various components of the atlas, which in turn will be used to initialize a multi-surface 2-Simplex, featuring shared boundaries where appropriate, by exploiting geometric duality. This multi-surface 2-Simplex

will then refine an atlas-to-image mutual-information maximizing registration through Gilles' gradient-aware Newtonian Simplex model. Some resampling may also be involved, to interpolate between consecutive slice images along the longitudinal axis.

Validation of printed-to-digital atlas transposition is still an open question. Because of the importance of the accuracy of the result, any error found in the minimally supervised result will certainly be manually corrected by a neuroanatomist. Validation of the multi-material contouring is still underway, and will ultimately involve the computation of geometric statistics that quantify the fidelity of the mesh surfaces to the underlying anatomical compartments of the 3D atlas.

As described above, we would like to develop a more robust version of this 2D processing as well as 3D stacking. The 2D version will have a 2D 1-Simplex, initialized with a closed contour, capture the underlying labeled contour, however sparsely defined with user-labeled broken lines. The resulting closed contour will be post-processed in the current manner that we do with the paint-by-numbers Fast Marching-based labeling, thereby producing a dense 2D label map. We also anticipate that the 2D 1-Simplex contour model might be involved in the inter-slice interpolation in conjunction with the sampling exercise. The 2-Simplex surface model will help impose 3D smoothness on the final result.

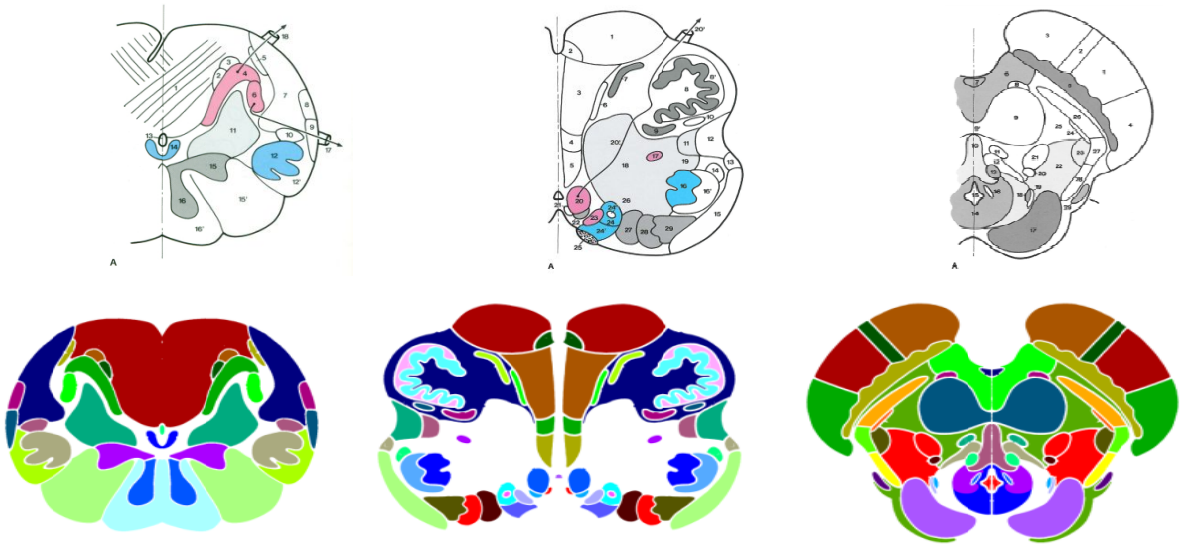

(a)

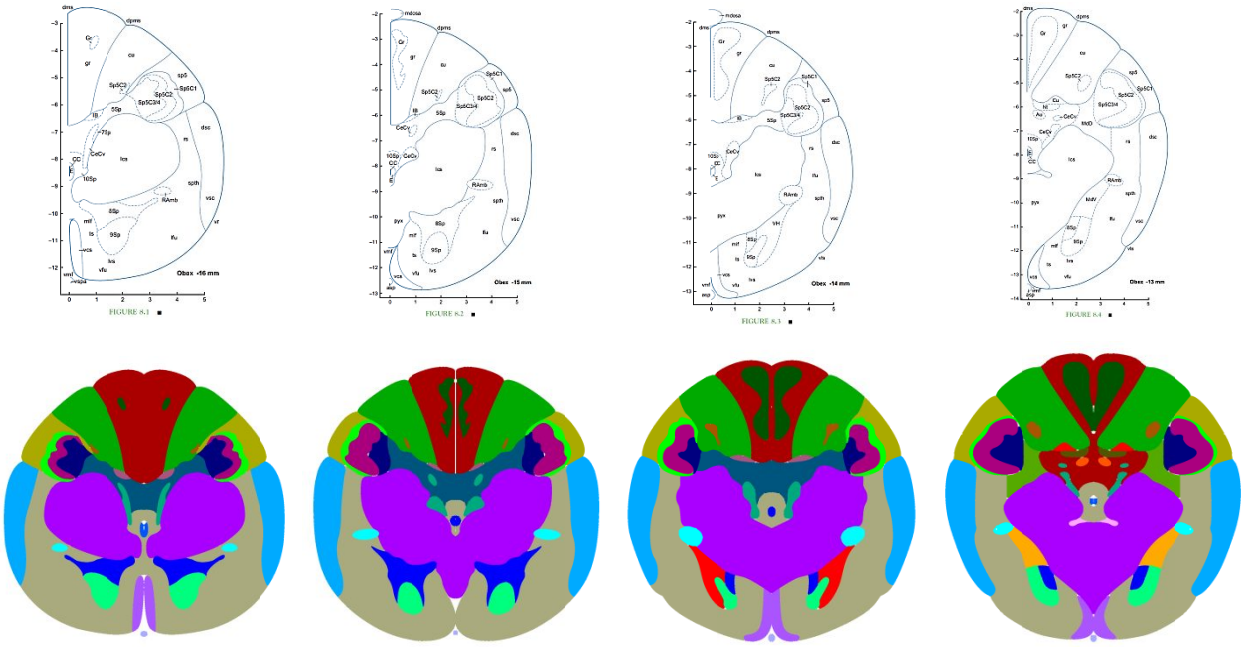

(b)

Figure 3. 2D contouring results from level-set contour based paint-by-numbers methodology. (a) Results for Duvernoy atlas; (b) results for Paxinos atlas, coinciding with slices 1 through 4.

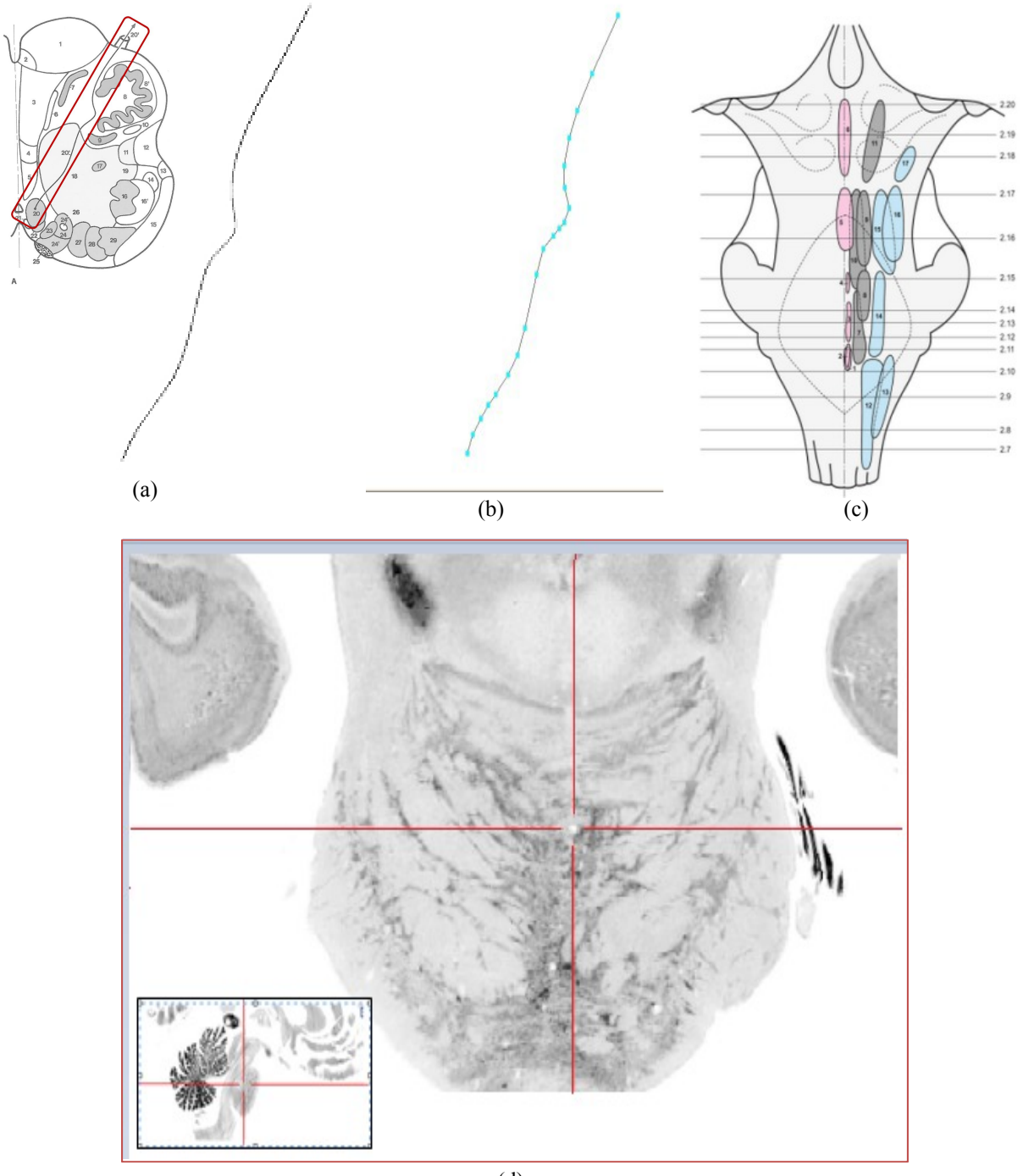

Figure 4. Modeling of cranial nerves: (a) Minimal Path-based models of cranial nerves in two scanned images; (b) 1-Simplex contour mesh of first MP in (a); (c) Z-coordinate of each 2D slice, based on published atlas illustration [5]; (d) coronal slice (inset: sagittal slice) of histological 100 μm MNI-space reformatted Big Brain dataset, emphasizing brainstem [16].

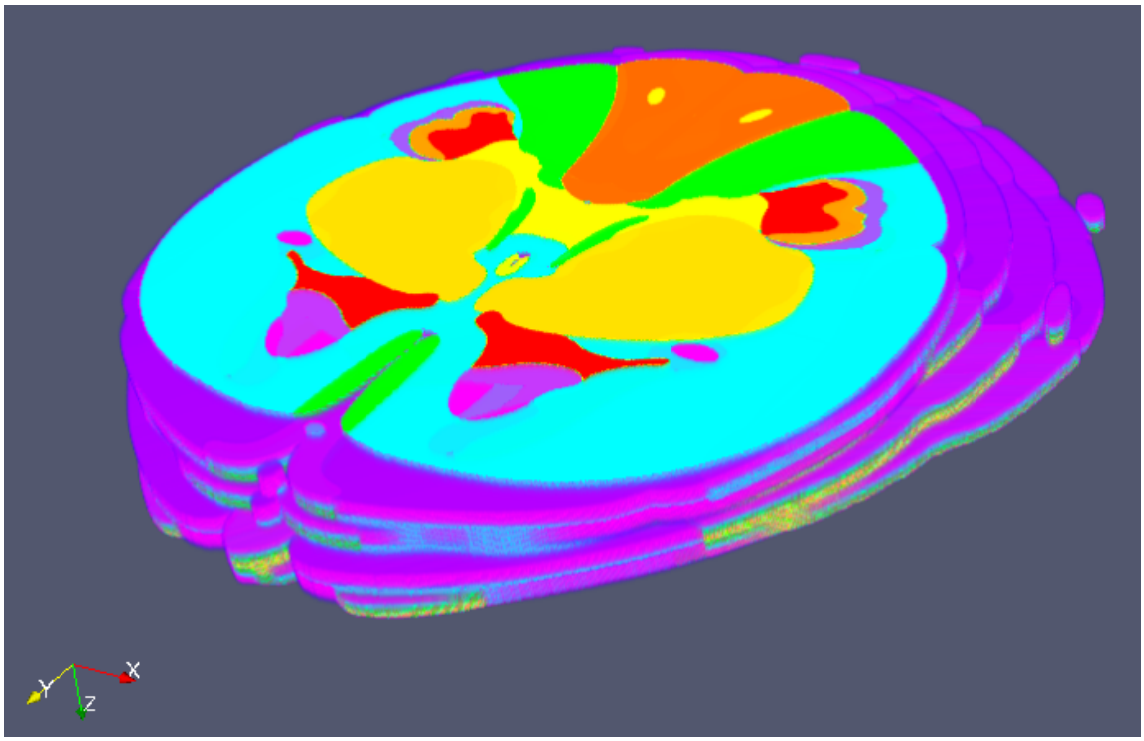

(a)

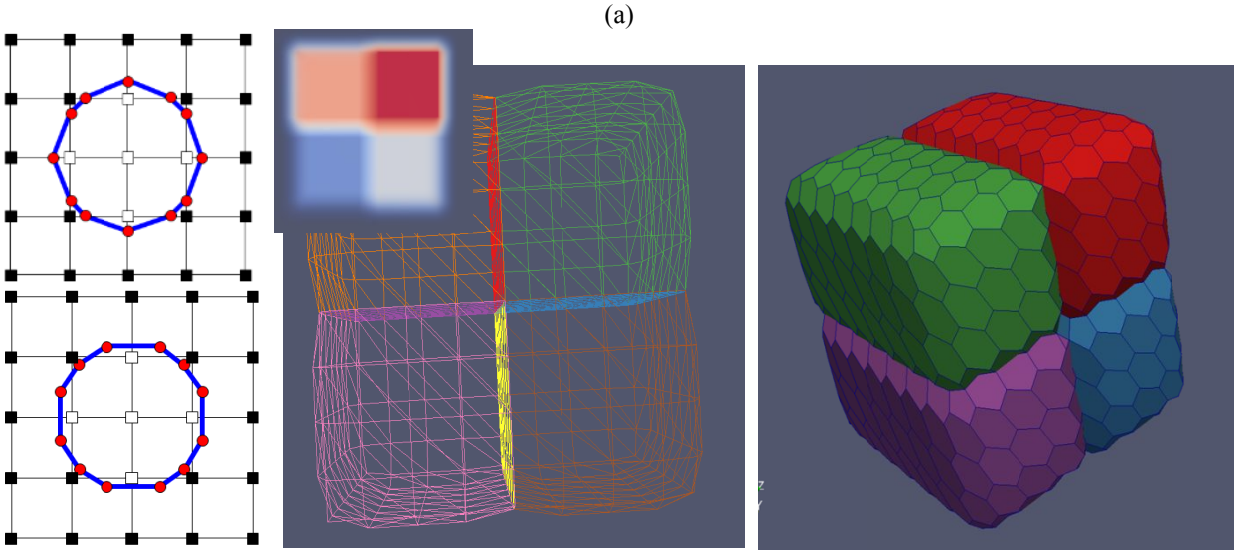

(b)

Figure 5. 3D processing- preliminary results. (a) Stacking of eleven slices consisting of digitized 2D label maps (not necessarily the same color map as figure 3), visualized with Paraview. (b) Multi-material dual contouring and multi-surface shared-boundary 2-Simplex. Left to right: (left) 2D Marching Squares-type contouring (top) and dual contouring (bottom); (center) multi-material dual contouring triangulated surface results of synthetic 4-compartment image (inset), with shared boundaries depicted in different colors; (right) shared-boundary four-compartment 2-Simplex mesh obtained by geometric duality from (b).

4. CONCLUSIONS

This paper presented on-going research on the development of a digital atlas of the brainstem. Applications of this digital atlas include the anchoring of cranial nerve contour models. The processing features both 2D and 3D stages, with this paper mostly presenting 2D results. We have demonstrated the method on two printed atlases, which each have their strengths. Our plan is to leverage the density of information of the Paxinos atlas along with the nerve contours made explicit in the Duvernoy atlas, and ultimately exploiting the MNI Big Brain data as well as 3D 1-Simplex and 2-Simplex models to refine the final discrete atlas. Future work also involves making this digital atlas probabilistically representative, using a series of high-resolution scans of the brainstem.

5. ACKNOWLEDGMENTS

This research was partially funded by the Jeffress Trust Foundation.

6. REFERENCES

[1] FSL. *Atlases. Templates and Atlases included with FSL.* . http://fsl.fmrib.ox.ac.uk/fsl/fslwiki/Atlases.
[2] Desikan RS, S.F., Fischl B, Quinn BT, Dickerson BC, Blacker D, Buckner RL, Dale AM, Maguire RP, Hyman BT, Albert MS, Killiany RJ., *An automated labeling system for subdividing the human cerebral cortex on MRI scans into gyral based regions of interest.* Neuroimage. , 2006 Jul 1: p. 31(3):968-80. Epub 2006 Mar 10.
[3] Fischl B, S.D., Busa E, Albert M, Dieterich M, Haselgrove C, van der Kouwe A, Killiany R, Kennedy D, Klaveness S, Montillo A, Makris N, Rosen B, Dale AM, *Whole Brain Segmentation: Automated Labeling of Neuroanatomical Structures in the Human Brain.* Neuron, 2002: p. 33:341-355.
[4] Mai JK 14, e.a., *Atlas of the Human Brain - Brainstem*.
[5] Naidich T, *Duvernoy's Atlas of the Human Brain Stem and Cerebellum*. 2009, Am Soc Neuroradiology.
[6] Paxinos G, Huang XF, Sengul G, Watson C, *Organization of brainstem nuclei, The Human Nervous System;* 260-327, Amsterdam, 2012, Elsevier Academic Press; available online at http://ro.uow.edu.au/cgi/viewcontent.cgi?article=4108&context=hbspapers .
[7] Shoja M, e.a., *A comprehensive review with potential significance during skull base and neck operations, Part II: glossopharyngeal, vagus, accessory, and hypoglossal nerves and cervical spinal nerves 1-4.* Clin Anat., 2014 Jan: p. 27(1):131-44.
[8] Gilles B, Magnenat-Thalmann N., *Musculoskeletal MRI segmentation using multi-resolution simplex meshes with medial representations.* Med Image Anal., 2010 Jun: p. 14(3):291-302. Epub 2010 Mar 1.
[9] Chan TF, Vese LA, *Active Contours without Edges,* IEEE Trans. Image Process., 2001, 10(2): 266-277.
[10] Caselles V, K.R., Sapiro G, *Geodesic active contours,".* Int. J. Comput. Vision, , 1997: p. vol. 22, pp. 61-79.
[11] Sethian JA, *A fast marching level set method for monotonically advancing fronts.* 1996. Vol. 93, pp. 1591-1595.
[12] Cohen, L.D. and R. Kimmel, *Global minimum for active contour models: A minimal path approach.* Int. J. Comput. Vision, 1997. 24(1): p. 57-78.
[13] Cohen, L., *Minimal paths and fast marching methods for image analysis*, in *Handbook of mathematical models in computer vision*. 2006, Springer. p. 97-111.
[14] Delingette H. "General Object Reconstruction Based on Simplex Meshes." Int. J. Comput. Vis. [1999]: 32(2):pp 111-146.
[15] Frangi AF, Niessen WJ, Vincken KL, Viergever MA. *Multiscale vessel enhancement filtering.* International Conference on Medical Image Computing and Computer Assisted Intervention, . vol. 1496 of Lecture Notes in Computer Science, , 1998. pp. 130-137.
[16] BigBrain. *Montreal Neurological Institute , BigBrain LORIS Database*. Available from: https://bigbrain.loris.ca/main.php.
[17] Y. Zhang and J. Qian, *Dual contouring for domains with topology ambiguity*, Computer Methods in Applied Mechanics and Engineering, vol. 217, pp. 34-45, 2012.
[18] Y. Zhang and J. Qian, *Resolving topology ambiguity for multiple-material domains*, Computer Methods in Applied Mechanics and Engineering, vol. 247, pp. 166-178, 2012.
[19] Tejos C, et al. *Simplex Mesh Diffusion Snakes: Integrating 2D and 3D Deformable Models and Statistical Shape Knowledge in a Variational Framework.* Int. J. Comput. Vision 85(1): 19-34 [2009]: 85(1): 19-34.